

REVIEW

[View Article Online](#)  
[View Journal](#) | [View Issue](#)



Cite this: *Inorg. Chem. Front.*, 2025, **12**, 2194

## Design, analysis, and application of metal–organic framework derived carbons

Joshua A. Powell, <sup>a,b</sup> Yihao Yang <sup>a</sup> and Hong-Cai Zhou <sup>a</sup>

Metal–organic framework-derived carbons (MOFdCs) have emerged as a rapidly growing class of porous materials over the past 15 years. Inspired by the principles of templated synthesis used in organic chemistry and nanomaterials, MOFdCs combine the highly tunable features of metal–organic frameworks with the versatility and stability of traditional porous carbon materials. Although many advances in MOFdC applications have been driven by an exploratory approach, there is a growing body of systematic, hypothesis-driven studies of the underlying chemistry and materials science of MOFdC structure, design, and structure–property relationships. This review summarizes developments in the systematic design and characterization of MOFdCs and strategies developed to control the structure of these materials. The role of variables such as pyrolysis temperature, gas environment, and the atomic- and nanoscale structure of the template MOF are described, with particular emphasis on their relationship to MOFdC structure and applications. By focusing on the fundamental principles underpinning MOFdC design, this work will lead to more rationally designed MOFdC materials and greater efficiencies in the development of MOFdCs for a host of applications.

Received 13th December 2024,  
Accepted 2nd February 2025

DOI: 10.1039/d4qi03205e

[rsc.li/frontiers-inorganic](http://rsc.li/frontiers-inorganic)

### Introduction

Porous materials are of growing importance in our society, as we seek highly efficient catalysts and adsorbents for energy storage and environmental remediation. Charcoal, a porous carbon material, has been described in sources from cultures

across the world from as early as 1500 BC and has been used for medicinal applications and water purification for centuries.<sup>1–4</sup> In the late 20<sup>th</sup> and early 21<sup>st</sup> centuries, chemists such as Robson, Yaghi, and Kitagawa introduced a new type of porous material, known as porous coordination polymers or metal–organic frameworks (MOFs).<sup>5–10</sup> These materials exhibited both permanent porosity and highly tunable structures and represented a significant advance in obtaining a high level of control over the structure of porous materials. Research over the last 25–30 years has expanded greatly on these early reports to produce MOFs that are more stable<sup>11–17</sup> and have

<sup>a</sup>Department of Chemistry, Texas A&M University, College Station, TX 77843, USA.

E-mail: [j.powell1@uq.edu.au](mailto:j.powell1@uq.edu.au), [zhou@chem.tamu.edu](mailto:zhou@chem.tamu.edu)

<sup>b</sup>School of Chemical Engineering, The University of Queensland, St Lucia, QLD 4072, Australia



**Joshua A. Powell**

design and application of thermally-transformed framework materials.

*Joshua Powell completed his BSc (Hons) in Chemistry at the University of Queensland in 2018 with Jack K. Clegg and completed his PhD in Chemistry at Texas A&M University in 2023 with Hong-Cai Zhou. Following a 12-month stint in industry performing commercial research and development of porous materials, he returned to the University of Queensland as a postdoctoral research fellow. His current research focuses on the*



**Yihao Yang**

*Yihao Yang received his B.S. degree in chemistry from Peking University, Beijing, China in 2017 and M.S. degree in chemical engineering from University of Southern California in 2020. He is currently a Ph.D. candidate in chemistry at Texas A&M University. His research is focused on modification and applications of metal–organic frameworks (MOFs), mainly on catalysis, gas separation and electronic conductivity.*

various functionalities apportioned throughout the framework structure.<sup>8,17–22</sup> However, despite the sophistication of these materials, their stability is often poor compared to more established porous materials, such as porous carbon or zeolites, thus limiting their applicability.<sup>23–27</sup> Consequently, the commercialization of MOFs has been limited to a small number of niche applications and the need for a highly controllable porous material remains.<sup>26–28</sup>

Templated synthesis is a key strategy by which structural control has been achieved in fields such as organic chemistry, biochemistry, and nanomaterials.<sup>29–37</sup> As their cost has decreased and their ease of synthesis has improved, MOFs have begun to be used as templates for the design and synthesis of new MOF-derived materials. One example of this is the advent of MOF-derived carbon (MOFdC) materials, which are porous carbons derived from the thermal decomposition of MOFs.<sup>37–40</sup> Some MOFdCs are also decorated with metal species derived from the inorganic components of the MOFs. Compared to their template MOFs, MOFdCs are typically much more thermally and chemically robust,<sup>37,38</sup> which provides greater opportunities for their application under working conditions for electrocatalysis and other industrial chemical processes.<sup>41–44</sup> Most importantly, the structure of the template MOF can be tuned or altered to impart specific properties into the MOFdC. By encapsulating guests inside the framework, doping the structure with additional metal ions to form bimetallic MOFs, or altering the connectivity or composition of the inorganic or organic building units, the structure of MOFdCs can be tuned in a fashion that is unusually controllable for an amorphous material.

## Early MOFdC development

Many early MOFdCs required the incorporation of additional carbon sources into the template framework to circumvent excessive loss of carbon through combustion. Xu and co-



Hong-Cai Zhou

he has been listed as a Highly Cited Researcher by Thomson Reuters every year, and in 2016 he was elected a fellow of the AAAS, ACS, and RSC.

workers reported one of the first MOFdCs, which was synthesized *via* carbonization of a polyfurfuryl alcohol@MOF-5 composite at 1000 °C under an argon atmosphere. Under these conditions, the organic linkers and polyfurfuryl alcohol were transformed into a porous carbon material with a high surface area.<sup>39</sup> Due to the high carbonization temperature and the low boiling point of zinc, no metal was retained in the MOFdC structure, although zinc oxide could be observed at lower carbonization temperatures. Notably, the carbon structure contained micropores, mesopores, and macropores. Later research has shown that the micropores in MOFdC structures are typically derived directly from the micropores of the template MOF.<sup>45</sup> Xu later extended this research to test the application of these materials as electrodes for supercapacitors.<sup>46</sup>

Following this seminal work, other researchers applied similar strategies to generate MOFdCs from other template MOFs. Furfuryl alcohol remained a popular additive and was later applied in the carbonization of zeolitic imidazolate frameworks (ZIFs) by several researchers (Fig. 1a).<sup>47,48</sup> Gao and coworkers studied the incorporation of various different carbon additives, including a phenolic resin, carbon tetrachloride, and ethylenediamine, finding that carbonization of additive-free MOF-5 produced a MOFdC with high porosity, while carbonization of MOF-5 with all three additives produced a more graphitic carbon.<sup>49</sup>

Eventually, MOF carbonization strategies that did not require the inclusion of an additional carbon source were developed (Fig. 1b). Around the time that Xu and coworkers published their MOFdC study, other researchers reported the synthesis of MOF-derived multiwalled carbon nanotubes,

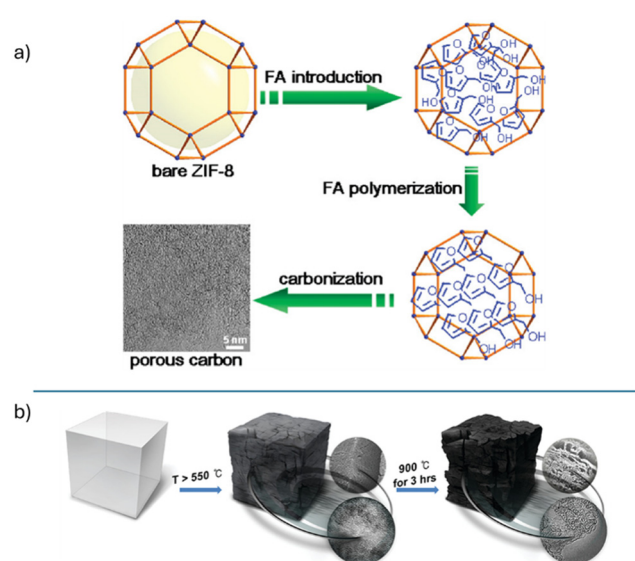


Fig. 1 (a) Incorporation of furfuryl alcohol prior to carbonization increases carbon content in the final MOFdC material. Reprinted with permission from ref. 47. Copyright 2011 American Chemical Society; (b) direct carbonization of MOF crystals can also be achieved. Reprinted with permission from ref. 54. Copyright 2012 American Chemical Society.



where the metal center of the MOF was used to catalyze the formation of the carbon structure.<sup>50</sup> However, examples of direct MOF carbonizations where the porous structure of the template MOF was retained did not arise until the early 2010s.

One of the earliest examples was the direct carbonization of an aluminium-based MOF by Yamauchi and coworkers.<sup>51</sup> The MOF in question had previously been carbonized with the addition of furfuryl alcohol,<sup>52</sup> however Yamauchi and coworkers found that the carbon content of the 1,4-naphthalene dicarboxylic acid linker was in fact sufficient to produce a carbon matrix with high porosity after the material was treated to remove the alumina nanoparticles derived from the inorganic building units (IBUs).<sup>51</sup> Notably, the carbonization temperature was a key variable that affected the porosity of the MOFdC, with carbonization at 800 °C producing the MOFdC with the highest surface area. At temperatures above 900 °C, the MOFdCs exhibited a drastic reduction in porosity due to graphitization and collapse of the carbon pore structure.

In contrast to the Al-MOF template described above, many MOFdCs are formed from Zn-MOFs, as the low boiling point of zinc metal leads to the removal of the metal species without any subsequent processing. Banerjee and Kurungot directly carbonized several zinc-based MOFs and coordination polymers to produce porous carbons that required no post-synthetic treatment due to the evaporation of the zinc. In an effort to maximize carbon content and surface area, this study explored a range of different linkers with varied lengths and aromaticity.<sup>53</sup> Park and coworkers also reported the direct carbonization of IRMOFs 1, 3, and 8 (IRMOF = isoreticular MOF). They were able to tune the pore size of the MOFdCs and optimize them for hydrogen uptake by altering both the structure of the template MOF and the pyrolysis temperature.<sup>54</sup>

One of the most popular MOF templates for the formation of MOFdCs is ZIF-8. This framework is comprised of zinc ions as IBUs and 2-methylimidazolate linkers that provide sufficient carbon content to form highly porous MOFdCs without the incorporation of additional carbon sources. Furthermore, ZIF-8 is both inexpensive and synthetically simple to produce in the quantities required for carbonization, as cost is a key limitation to the commercialization of MOFs and MOFdCs.<sup>47,55–59</sup>

As the field of MOFdCs has begun to mature, more complex MOFdC structures are being generated. While some MOFdC research remains focused on simple porous carbon structures, many researchers have begun to synthesize MOFdCs with N- or S-doped carbons or containing metal species derived from the template MOF.<sup>47,60</sup> These more complex structures represent a significant advance in the versatility of MOFdCs, as they provide several additional structural variables that can be tailored to form materials with specific structures or functionalities.

## Structural features of MOFdCs

There is a great deal of diversity in the structure of MOFdCs, however there are several features that are common to many MOFdCs (Fig. 2). First is the presence of a porous carbon

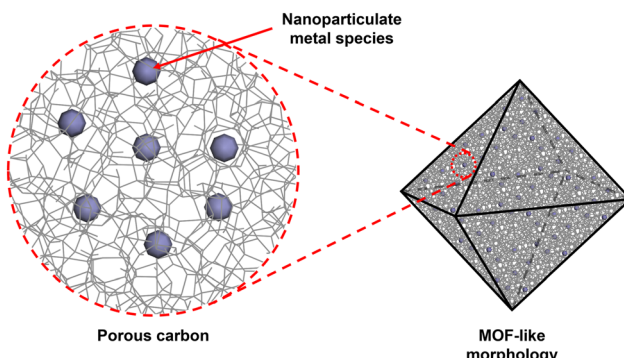


Fig. 2 Schematic of MOFdC structural features showing MOF-like morphology, porous carbon, and nanoparticulate metal species.

matrix, which is a universal feature in these materials.<sup>46,49,52,61–63</sup> Originally derived from a combination of the organic linker and additional carbon-containing guests, and later from the organic linkers alone, the structure of this porous carbon is strongly related to the structure of the template MOF. The carbon typically contains a mixture of micropores and mesopores, the sizes of which are derived from the pores of the original MOF template.<sup>45,49,52,64</sup> Pore size distributions of MOFdCs obtained *via* gas sorption analysis show that the micropores in the carbon are of the same size as the micropores in the MOF. The mesopores are generated by a combination of combustion of the organic components and *in situ* defect formation leading to partial structural collapse during the carbonization.<sup>45,64–66</sup> The relative concentrations of micro-*versus* mesopores can be tuned based on the pyrolysis conditions. Harsher carbonization conditions, such as high temperatures or oxidizing gas environments, lead to the formation of greater mesoporosity, as the harsh conditions generate more defects in the MOF during the pre-carbonization heating and encourage a greater degree of combustion of the organic components. Depending on the composition of the organic linker or organic additives, the carbon matrix can also have additional elements doped into the non-graphitic carbon structure. Most common is nitrogen-doping, which is achieved by either including a nitrogen-rich guest like urea in the MOF prior to carbonization<sup>60,67</sup> or by designing a MOF structure with nitrogen-rich linkers, such as the ZIF-8/ZIF-67 system.<sup>47</sup> Carbonization of these nitrogen-rich templates produces N-doped carbon, which enhances the energy storage properties and the electrochemical activity of the material.<sup>40,47,61,62,68</sup> MOFdCs with sulfur-doped and phosphorus-doped carbons have also been reported, however these are less common.<sup>69</sup> MOF-derived materials that do not contain a carbon matrix can also be generated,<sup>70–72</sup> however these materials are outside the scope of this review.

On a macro scale, MOFdCs also inherit structural features from the template MOFs. As highly ordered crystalline materials, MOFs generally grow in well-defined morphologies, such as octahedra, cubes, or rods. Upon carbonization, these morphologies are well-maintained, with MOFdCs usually exhibiting the same morphology as the template MOF



crystals.<sup>40,73,74</sup> Due to the loss of material through partial combustion or evaporation of the metal species, the faces of octahedral or cubic MOFdCs are often sunken in.<sup>75</sup> Furthermore, due to the loss of relatively strong coordination bonds in three dimensions and the generation of additional grain boundaries, MOFdCs are generally more brittle than the template MOFs.<sup>76</sup>

Another feature that is common, though not universal, in MOFdCs is the presence of inorganic components. While some MOFdC research focuses on the structure of the carbon components and will deliberately remove the inorganic components,<sup>51,52</sup> the field of metal-containing MOFdCs is growing rapidly.<sup>37,68,77–79</sup> Inorganic components typically exhibit nanosized domains, as the temperatures of MOF pyrolysis are often not high enough to melt or sinter the metal species into larger domains.<sup>80,81</sup> In some cases, the inorganic species are single atoms supported on the carbon,<sup>62,77,82</sup> however this is often difficult to achieve due to the high temperatures of the carbonization and the close proximity of the metal ions in the template MOF structure. A variety of metal species can be formed in a MOFdC, including metals, metal oxides, metal nitrides, metal carbides, and metal sulfides.<sup>45,79,83–87</sup> In cases where more than one metal ion is contained within the IBU or hosted in the pores of the MOF, multimetallic inorganic species or alloys are often formed.<sup>88–92</sup> Due to the small size of the domains and inorganic node distortions that occur upon heating, metal species in MOFdCs are often poorly ordered, which makes traditional bulk scale or average structure analysis challenging or poorly representative of the true structure of the species.<sup>83,84,93–95</sup> Consequently, many researchers in the field have relied on local structure analysis techniques, such as X-ray or neutron total scattering or extended X-ray absorption fine structure (EXAFS) to complement average structure analysis.<sup>45,83,84,94–96</sup>

## Effect of carbonization conditions on MOFdC structure

More recently, research into the influence of carbonization conditions on the MOFdC structure and composition has begun to be studied. An early work in this area was performed by Banerjee, Poddar, and coworkers, who compared carbonization of a range of MOFs in both air and nitrogen environments. They found that the inorganic species produced from carbonization in air exclusively formed metal oxides, regardless of the identity of the metal ( $M = \text{Mg, Mn, Co, Cu, Zn, Cd}$ ). However, carbonization in nitrogen produced metallic nanoparticles of cobalt and copper, while the other metals were not reduced under these conditions due to their lower oxidation potential.<sup>87</sup>

In another such study, Zhou and coworkers conducted a detailed investigation of the iron MOF PCN-250 (PCN = porous coordination network) and the effects of pyrolysis temperature and gas environment on the structure of the resulting iron species and carbon matrix in the MOFdC (Fig. 3).<sup>45</sup> They found that pyrolysis in oxidizing gases produced MOFdCs with

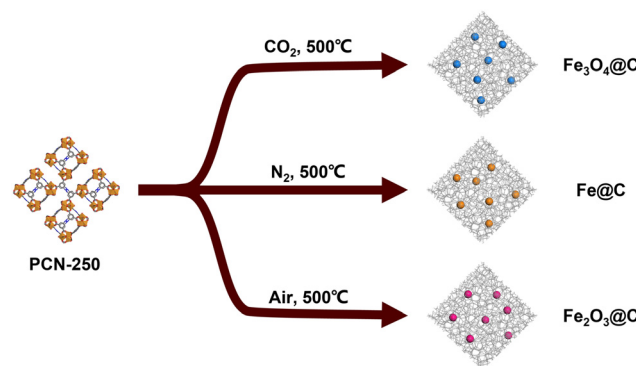
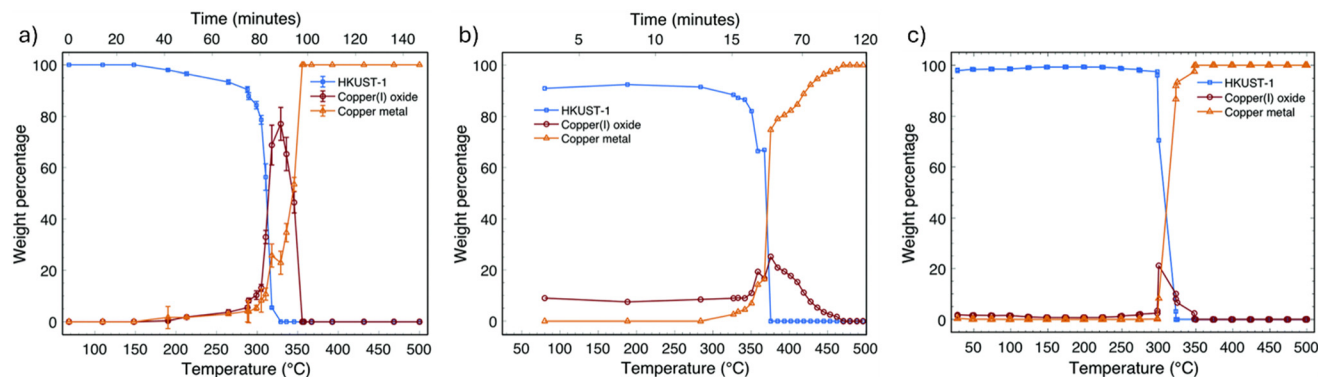


Fig. 3 Influence of MOF pyrolysis conditions on the structure of PCN-250-dC.

low surface areas and low carbon content, suggesting that the oxidative conditions caused combustion of the linker before it could be carbonized. In contrast, non-oxidizing atmospheres typically produced much higher surface areas and higher carbon content, suggesting that a non-oxidizing environment is key for retaining the porous structure of the MOF after carbonization. Chapman and coworkers similarly investigated the pyrolysis of PCN-250 under reducing atmospheres, corroborating the results reported by Zhou and expanding the scope of the research to consider the structure of metal oxide nanoparticles derived from multimetallic PCN-250.<sup>94</sup> Zhou and coworkers also demonstrated that the linker decomposition process involves an oxidative decarboxylation, which in turn reduces the iron of the MOF cluster to iron(0) before later being oxidized, while Chapman and coworkers identified metal node distortions prior to structural collapse, suggesting that both node and linker dynamics contribute to the MOF decomposition.<sup>45,65,66,94</sup> This process also shed light on differences in the iron oxide phase present following pyrolysis in different gas environments. While carbonization in oxidizing gases produced a single phase of iron oxide due to uniform oxidation of the iron(0) intermediate during the carbonization, carbonization in non-oxidizing gases produced multiple iron oxide phases due to the  $\text{CO}_2$  produced during the carbonization and post-carbonization oxidation upon exposure to ambient air.<sup>45</sup> Carbonization in more strongly reducing gas environments produced iron(II) oxide, perhaps by inhibiting the oxidative decarboxylation of the linker.<sup>94</sup> Notably, this mechanistic understanding of the carbonization process has subsequently been applied to target the formation of MOFdCs with specific structural features.<sup>97</sup> Cheetham, Wang, and coworkers also observed the effect of gas environment on the metal species of a MOFdC. Carbonization of a manganese triazolate framework under rigorously oxygen-free conditions produced nanoparticulate manganese nitride that was air-stable, a property not found in bulk manganese nitrides. In contrast, carbonization in air produced manganese oxide.<sup>83</sup> As the nitrogen of the manganese nitride was derived directly from the triazolate linker, this suggests that different reaction mechanisms may be at play depending on the gas environment.





**Fig. 4** Evolution of MOF, Cu(i) oxide, and Cu(0) phases during carbonization of HKUST-1, as measured by XAS (a), X-ray PDF (b), and PXRD (c). Reproduced from ref. 96 with permission from the Royal Society of Chemistry.

Zhou and coworkers also noted some significant differences in MOFdC structure based on pyrolysis temperature. When Zn-MOF-74 was carbonized below 600 °C, ZnO nanoparticles were produced, while carbonization above 600 °C caused sintering of the ZnO into a bulk domain.<sup>84</sup> This sintering causes an increase in mesoporosity as the ZnO sinters to the exterior of the MOFdC, leaving mesoporous voids on the interior of the material. While this specific sintering behavior had not been previously observed in MOFdCs, other temperature dependent effects have been described. The first MOFdC reported was calcined at 1000 °C to ensure evaporation of the zinc species derived from the IBU, however it was also possible to obtain zinc oxide-containing MOFdCs by carbonization at lower temperatures, albeit at the expense of high porosity.<sup>39</sup> The rate of heating can also influence this sintering behavior. More rapid heating ramps typically produce larger, more crystalline metal species, as the activation energy for grain growth can more readily be overcome.<sup>98,99</sup> Notably, the effect of heating ramp is generally negligible on the decomposition pathways or the identity of the final metal species, as demonstrated by pyrolysis of HKUST-1 (HKUST = Hong Kong University of Science and Technology) at heating ramps from 2–5 °C min<sup>-1</sup> (Fig. 4).<sup>96</sup> By conducting *in situ* powder X-ray diffraction (PXRD), X-ray absorption spectroscopy (XAS), and X-ray total scattering pair distribution function (PDF) experiments, the authors observed that the MOF decomposed at 300–325 °C into a mixture of Cu(0) and Cu(i) oxide, the latter of which was an intermediate that was subsequently reduced to Cu(0) at higher temperatures (above 350 °C). While the Cu(i) oxide intermediate was not observed upon rapid heating (over 2500 °C min<sup>-1</sup>), this difference was ascribed to the limited time/temperature resolution that could be achieved in the analysis and does not necessarily indicate a change to the mechanism of Cu(0) formation.<sup>96</sup>

## Effect of MOF template structure on MOFdC structure

In addition to the carbonization conditions, features of the MOF template structure such as dimensionality, IBU structure,

and connectivity also play a role in determining the structure of the MOFdC. When comparing the carbonization products of copper MOFs HKUST-1 and F-MOF-4 (F-MOF = fluorinated metal-organic framework), the 3-dimensional HKUST-1 produces larger copper particles than the 2-dimensional F-MOF-4.<sup>87</sup> This enhanced growth was hypothesized to be a consequence of the dimensionality, as the HKUST-1-derived copper particles are agglomerated from all three dimensions. This hypothesis also held for the comparison between the 2-dimensional cobalt MOF MOF-CJ4 and the 3-dimensional cobalt MOF Co-HFMOF-D (HFMOF = partially fluorinated metal-organic framework).<sup>87</sup>

The effect of linker structure on the pore structure of the carbon matrix of the MOFdC has also been investigated. In another study, several zinc MOFs with a range of linkers were carbonized to produce metal-free MOFdCs of varied structure. Carbonization of MOF templates with more rigid and aromatic linkers produced porous carbons that maintained the morphology and pore structure of the template MOF, while more flexible linkers produced carbons with much less well-ordered pore structures.<sup>53</sup>

The influence of MOF structure on the resulting MOFdC was further explored by Zhou and coworkers. When comparing pyrolysis of Zn-MOF-74 and UiO-66 (UiO = University of Oslo), they found that carbonization of Zn-MOF-74 and its higher connected and more thermally stable linker produced MOFdCs with higher surface area by preventing pre-carbonization pore collapse.<sup>84</sup> Furthermore, they found that carbonization of UiO-66 produced primarily cubic zirconia due to the templating effect of the cubic Zr<sub>6</sub>-oxo clusters, despite this phase typically being considered unstable at particle sizes above 2 nm.<sup>100</sup>

Cheetham, Wang and coworkers note that while oxygen-free carbonization of a manganese triazolate framework produces manganese nitride, carbonization of the analogous iron and cobalt triazolates under the same conditions produce iron carbide and cobalt metal respectively.<sup>83</sup> While this was not explored in depth, it further emphasizes that different inorganic components in the MOF can result in different reac-



tion pathways and different inorganic products. Likewise, Zhou and Chapman have both demonstrated that incorporation of a heterometal into the cluster of PCN-250 can produce different metal phases following carbonization, with PCN-250-Fe<sub>2</sub>Ni in particular favoring the formation of fcc-Ni due to the favorability of FeNi alloy formation and selective Ni extraction from the cluster during the pyrolysis process.<sup>94,97</sup>

One of the most significant advances in MOFdCs in the last decade is the development of the metal ion “fence” strategy to form MOF-derived single atom catalysts (SACs) supported on a porous carbon matrix (Fig. 5). Following reports of Co SACs formed from bimetallic ZIF structures,<sup>101,102</sup> this strategy was more systematically developed by Wu, Li, and coworkers, who carbonized a mixed cobalt/zinc ZIF to produce single cobalt atoms anchored to a N-doped carbon matrix.<sup>77</sup> By incorporating zinc ions in the ZIF structure as a “fence” between cobalt ions, the cobalt ions were too spatially separated to undergo significant aggregation and thus remained embedded as single atoms in the carbon with a porphyrinic planar structure. Wang and coworkers further investigated the relative activity of MOF-derived Co-SACs and MOF-derived cobalt nanoparticles for nitroarene hydrogenation, showing that the SACs were significantly more active.<sup>103</sup> This fencing strategy has since been used with other metal dopants, including iron,<sup>62,104–107</sup> manganese,<sup>104</sup> nickel,<sup>107–110</sup> and copper.<sup>110,111</sup>

An alternative strategy that relies on the same principle is that described by Zhou, Li and Fischer, in which the porphyrin center of a porphyrinic zirconium-based MOF was partially metalated with nickel and several other transition metal ions.<sup>82</sup> As with the fence strategy, the incomplete metalation of the porphyrin center resulted in significant distance between the nickel ions and prevented agglomeration or sintering into larger particles upon carbonization of the MOF, instead producing SACs on a porous carbon support. However, this strategy is not universally applicable. When a zinc-porphyrin MOF metalated with palladium is used in place of the zirconium-porphyrin MOF metalated with nickel, the final material con-

tained a palladium-zinc alloy instead of single palladium atoms dispersed on the carbon.<sup>112</sup>

More complex metal species can be produced by designing MOF templates with more than one metal ion in the IBU. Prussian blue, a coordination polymer known since the early 1700s, can be calcined to form porous multimetallic iron oxide structures, with partial substitution of the iron atoms by heterometals such as manganese or cobalt.<sup>90,91</sup> Another popular MOF template for the formation of alloys is M-btc ( $\text{H}_3\text{btc}$  = benzene 1,3,5-tricarboxylic acid), as multimetallic MOFs of this structure can be readily synthesized in one-pot reactions simply by varying the concentration of each respective metal ion in the reaction mixture.<sup>88,89</sup>

It is also possible to incorporate secondary metals by impregnating the MOF with the metal or metal precursor prior to carbonization. This strategy has commonly been performed with the ZIF-8/ZIF-67 system, as techniques for impregnation of metal nanoparticles in this MOF are well-established. This is a particularly desirable strategy when the metal of interest is too expensive to be used as the backbone of the MOF, for example noble metals such as gold or platinum.<sup>113,114</sup> In many cases, this strategy is used to form alloys or multimetallic species that are more active than the individual metals alone.<sup>92,114–117</sup>

## Structure–function relationships in MOFdCs

### Gas storage

As with most materials, the functionality of MOFdCs is dictated by their structure. Inspired by the promise of MOFs in gas storage applications, early work with MOFdCs similarly focused heavily on the gas storage properties of the materials. The first report of a MOFdC involved a discussion of the hydrogen uptake properties of the material,<sup>39</sup> which remained a popular application for MOFdCs throughout the early 2010s.<sup>47,54,87</sup> Crucially, MOFdCs outperformed porous carbons produced by other methods due to the high concentration of ultramicropores.<sup>54,118</sup> Furthermore, some highly graphitic MOFdCs are excellent materials for sensing aromatic compounds due to their high surface area and the affinity of the graphitic  $\text{sp}^2$ -hybridized carbons for aromatic molecules.<sup>51</sup> MOFdCs have also been used as sorbents for liquids and some dyes due to the hydrophobicity of the carbon and their high porosity.<sup>75,119–122</sup> In addition to their high uptake of oil and dyes, the presence of magnetic cobalt- or iron-based nanoparticles derived from the MOF IBUs can significantly improve recovery and recyclability of the sorbent.<sup>75,119</sup>

### Catalysis

MOF-derived bimetallic metal species have also been used as Fenton catalysts, where peroxide and hydroxide radicals are generated to degrade organic pollutants.<sup>123</sup> Similarly, MOF-derived SACs, often formed using the fencing strategy, have also been applied as Fenton or Fenton-like catalysts,<sup>106,124</sup> as

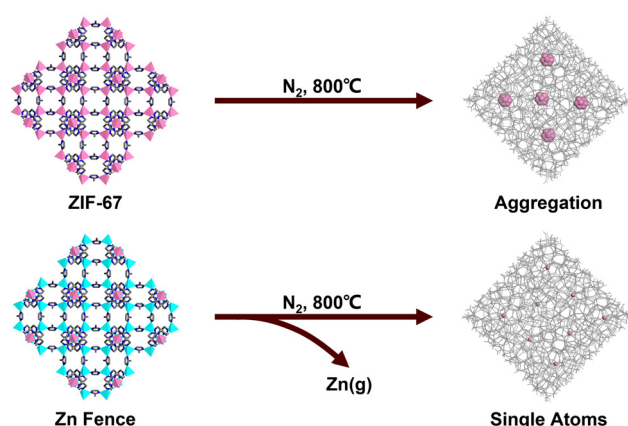


Fig. 5 “Fencing” strategy for the generation of ZIF-derived Co-SACs. The procedure is generalizable to other metals.



have MOF-derived cobalt nanoparticles<sup>125</sup> and partially carbonized Ce-TCPP nanocomposites (H<sub>4</sub>TCPP = tetrakis(4-carboxyphenyl)porphyrin).<sup>126</sup> Even metal-free MOFdCs have been applied as catalysts for peroxydisulfate activation due to the high activity of nitrogen-doped carbon structure.<sup>55,56</sup>

MOFdCs are also strong candidates for large-scale industrial catalysis at elevated temperatures and pressures.<sup>41,42,127,128</sup> Fischer-Tropsch synthesis of hydrocarbon chains from syngas is an important industrial reaction which is typically performed at high temperatures and pressures.<sup>41</sup> While MOFs may not be stable under these conditions, MOFdCs are significantly more resistant to high temperatures.<sup>37</sup> A variety of iron- and cobalt-based MOFs have been carbonized and applied for Fischer-Tropsch catalysis, with either ultrasmall metal nanoparticles or SACs as the active species. Gascon and coworkers have produced several iron-based MOFdCs that equal or outperform commercial Fischer-Tropsch catalysts.<sup>42,127</sup>

### Electrocatalysis

Due to the high concentration and good dispersion of metal species and the conductivity of the porous carbon matrix, MOFdCs have also shown significant promise as electrocatalysts for a variety of reactions. This review will briefly summarize several key reactions for which MOFdCs have been used as catalysts and the types of MOFdCs that have been applied in this way. Readers are directed to other recent reviews for a more detailed discussion of the design and application of MOFdCs for electrocatalysis.<sup>61,68,129–132</sup>

Electrochemical nitrogen reduction is an important reaction for energy storage as it presents a key avenue for hydrogen fixation and ammonia production. MOFdCs have recently been applied in this process.<sup>132,133</sup> In one such example, Cu-btc was calcined at several different temperatures to produce either a Cu-SAC or copper nanoparticles. The Cu-SACs were highly effective at promoting nitrate reduction while suppressing the accumulation of toxic nitrite ions.<sup>134</sup> Li and coworkers similarly found cobalt-doped iron nanoparticles derived from MOF-74 were effective nitrate reduction catalysts.<sup>135</sup> Nitrate is not the only substrate that has been converted to ammonia by MOF-derived catalysts. A bismuth-based MOFdC was used to fix nitrogen under ambient conditions with very high faradaic efficiency.<sup>136</sup>

Carbon dioxide utilization is another key process for which MOFdCs have been applied as electrocatalysts. The ZIF-8 system is a popular template for this reaction due to the propensity to form SACs upon carbonization. Both monometallic Ni-SACs and tandem systems that include Ni-SACs and either Cu- or Fe-SACs within the same porous carbon have been generated.<sup>107,108,110</sup> Other nickel-based MOFs have also been carbonized to produce Ni-SACs with promising results.<sup>88,137</sup> Similarly, HKUST-1-derived Cu-C composites have been applied for CO<sub>2</sub> electroreductions to both methanol and ethanol with high faradaic efficiencies and very low overpotentials (Fig. 6).<sup>138</sup> Titanium-based MOFs have also been applied as templates for the generation of carbon dioxide reduction

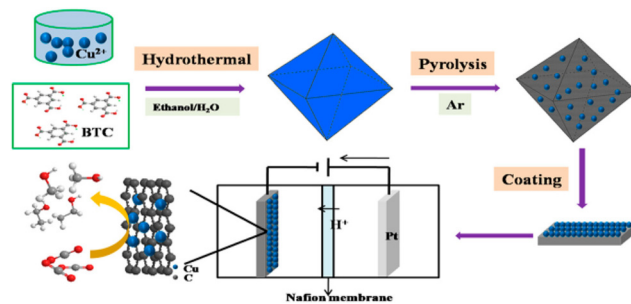


Fig. 6 Synthesis and utilization of HKUST-1-derived Cu-C composites for CO<sub>2</sub> electroreduction to C<sub>1</sub> and C<sub>2</sub> alcohols. Reprinted with permission from ref. 138. Copyright 2017 American Chemical Society.

reaction (CO<sub>2</sub>-RR) catalysts. In one example, MIL-125-derived Mg-doped titania (MIL = Materials Institute Lavoisier) was used to photocatalytically reduce carbon dioxide, with the magnesium dopant promoting the generation of surface Ti<sup>3+</sup> ions to improve charge separation. Furthermore, the Mg-doping increased the surface area of the titania by discouraging sintering.<sup>139</sup> In another, a mixed titanium-iron MOF was used to generate titanomaghemit nanoparticles with a high Fe/Ti ratio that cannot be achieved *via* traditional inorganic synthetic methods. This MOFdC was also an effective electrocatalyst for CO<sub>2</sub>-RR.<sup>140</sup>

Electrochemical water splitting reactions are also an important target reaction for MOFdC catalysts. Oxygen reduction reactions (ORR) are one of the most common applications in the literature for metal-containing MOFdCs.<sup>44,61</sup> While early work in this area focused on the generation of iron nanoparticles,<sup>141</sup> the ZIF-8/ZIF-67 system later became a popular template for the synthesis of these catalysts due to its propensity to form SACs, a consequence of the high nitrogen content in the carbon matrix and the ability to “fence” the Co ions with zinc in a bimetallic framework.<sup>77,105,142–144</sup> Cobalt is generally the most active SAC for these reactions, however iron and copper sites have also been employed.<sup>105,145</sup> Other MOFs have also been used as templates for generating SACs as ORR catalysts, such as Fe-doped NH<sub>2</sub>-MIL-101(Al).<sup>146</sup> These materials have been found to exhibit higher ORR activity than commercial Pt/C catalysts, representing an important step towards reducing society’s reliance on noble metals and increasing the sustainability of ORR.<sup>105,147</sup>

In addition to ORR, MOFdCs have been employed as multifunctional catalysts that are active towards both ORR and oxygen evolution reactions (OER), the latter of which is significantly more challenging due to its slow kinetics.<sup>43,44,68,148</sup> A diverse range of template MOFs have been used to generate such catalysts. In one example, a Zn-MOF was used as a host for copper or platinum nanoparticles and was carbonized to form a nanoparticle@porous carbon material without the inclusion of IBU-derived nanoparticles.<sup>149</sup> More common, however, is the generation of IBU-derived nanoparticles, such as through the carbonization of thiourea@Fe-btc to form an FeS/Fe<sub>3</sub>C@C composite or the carbonization of a cobalt-

vanadium mixed-metal MOF to form cobalt and vanadium nitride nanoparticles.<sup>85,86</sup>

### Energy storage

Finally, energy storage has recently emerged as an application for MOFdCs due to their high specific capacity, high surface area, and robustness towards volume expansion of guest materials.<sup>79,150,151</sup> Importantly, the porous carbon of MOFdCs is often graphitic in nature, thus the materials can be engineered to exhibit high capacities and enhanced ion transport compared to non-porous graphite.<sup>84,152,153</sup> These properties mean that MOFdCs often excel as anode materials for lithium, potassium, and sodium ion batteries.<sup>151–157</sup>

The conductive nature of the carbon also allows MOFdCs to be used as matrices for other high-capacity anode materials.

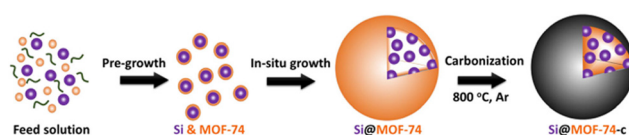


**Fig. 7** Synthesis of Si@MOFdC composite anode materials. Reprinted with permission from ref. 150. Copyright 2023 American Chemical Society.

Silicon anode lithium ion batteries are highly desired due to the extremely high theoretical capacity (4200 mA h g<sup>-1</sup>), however challenges such as volumetric expansion upon lithiation limit the amount of silicon that can be incorporated without experiencing severe capacity fade.<sup>158–160</sup> Several studies have demonstrated the utility of MOFdCs as a porous carbon host for nanoparticulate silicon (Fig. 7).<sup>150,160–162</sup> The high porosity of the carbon structure enables highly efficient lithium ion diffusion, leading to high specific capacity and high capacity retention.<sup>161</sup> Furthermore, the mechanically flexible porous carbon structure of the MOFdC mitigates the detrimental effects of silicon expansion, due to the porous carbon acting as a buffer to reduce strain or induce *in situ* formation of ultrasmall silicon nanodots.<sup>150,160</sup>

## Conclusions and outlook

MOFdCs are an attractive alternative to MOFs due to their enhanced stability and conductivity, and an improvement upon traditional porous carbons due to their microporosity and tunability. As demonstrated in this review, a vast array of MOFdC structures can be selectively synthesized through strategies such as judicious choice of carbonization conditions,

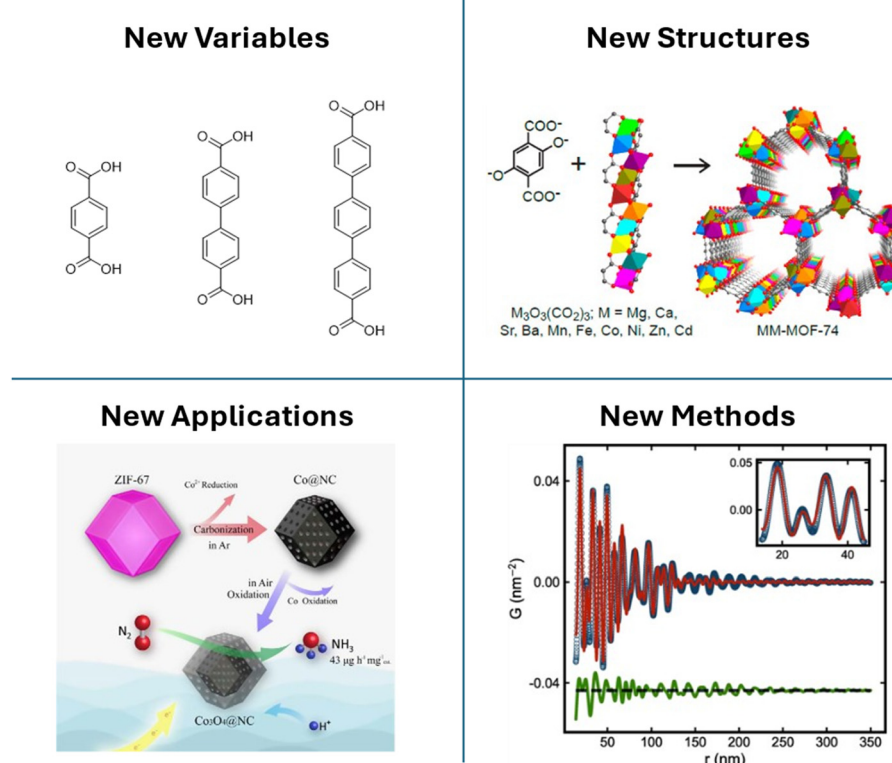


**Fig. 8** Future directions for MOFdC research include investigation of previously unstudied structural variables (e.g. linker length, top left), targeted design of multimetallic inorganic structures using multimetallic MOF platforms (top right, reprinted with permission from ref. 167. Copyright American Chemical Society 2014), targeted design of electrocatalysts at commercial scale (bottom left, reprinted with permission from ref. 133. Copyright American Chemical Society 2019) and use as a model system for developing advanced analytical techniques (e.g. sasPDF, bottom right, reproduced from ref. 169 with permission from the International Union of Crystallography).



tuning the MOF structure, and incorporating guests in the MOF prior to carbonization. As the field of MOFdCs continues to grow, there are a number of areas ripe for future research (Fig. 8).

While the literature to date has focused primarily on the templating effect of the IBU and framework structure and the impact of pyrolysis conditions, there are many other variables that have yet to be considered in the design of MOFdCs. Variables such as linker aromaticity and rigidity have been studied for their influence on the carbon structure,<sup>53</sup> however their impact on the structure of the metal species has not been considered. Other factors, such as linker length and connectivity, have not yet been systematically studied for closely related MOF templates, such as isoreticular expansions of a template MOF.<sup>11,163</sup> The inclusion of additional functional groups on linkers also provides a pathway for altering the structure of the metal species in the MOFdC, as they may interact differently with various chemical moieties throughout the carbonization process.<sup>93,164</sup>

MOFdCs also represent a step forward in the applicability of MOF-based materials due to their improved stability over the template MOFs. To this end, future research should consider the design of MOFdCs tailored to specific applications by using these principles. As electrocatalytic applications are widely investigated, future studies should employ systematic approaches to develop highly active, but inexpensive MOF-derived electrocatalysts, for example using bimetallic MIL-100(Fe) as a template instead of the more costly PCN-250.<sup>44,97,165,166</sup> Additional developments, such as the design of trimetallic (or more) MOFs as precursors for new and unusual inorganic materials, should also be pursued.<sup>140,167</sup>

Finally, MOFdCs provide a fascinating platform for the development of new analytical techniques and the advancement and extension of existing techniques. The nature of MOFdCs as poorly ordered solid materials that may contain regions of greater structuring, such as metal nanoparticles, challenges our existing conceptions on how to study the structure of materials. A swathe of advanced complementary techniques is required to fully describe the structure of MOFdCs and new techniques may be able to extract information from unexpected places. Given the often small size of the inorganic nanoparticles in MOFdCs, the combination of small- and wide-angle X-ray scattering (SAXS and WAXS) would provide an avenue to study the coevolution of X-ray scattering and Bragg diffraction peaks *in situ*, thus supporting models derived from other advanced *in situ* techniques.<sup>96</sup> Due to the differences in intensity of the scattering and diffraction features and the challenges of simultaneous detection across wide q-ranges, this type of analysis will inspire novel approaches in detector design and data collection methods that can be similarly applied in characterization of other advanced materials. Other cutting-edge techniques, particularly in the realm of local structure analysis, can also be further developed using MOFdCs as a model system. Due to their poor crystallinity, proper characterization of MOFdCs often requires the use of local structure analysis techniques, such as PDF or far-infrared

(terahertz) spectroscopy.<sup>45,94,168</sup> While it is possible to collect this type of data using conventional instrumentation, the cost and time required to obtain high quality data typically necessitates the use of synchrotron radiation. As the field of MOFdCs continues to grow, it will spur further advances in high-intensity X-ray sources and high-resolution detectors to enable greater accessibility, as well as the development of other advanced local structure analysis techniques, such as small angle scattering PDF (sas-PDF) and single-atom-sensitive electron energy loss spectroscopy (EELS).<sup>169,170</sup>

## Author contributions

J. A. P. and H.-C. Z. conceptualized the manuscript, J. A. P. and Y. Y. prepared the manuscript, H.-C. Z. conducted supervision.

## Data availability

No primary research results, software or code have been included and no new data were generated or analysed as part of this review.

## Conflicts of interest

There are no conflicts to declare.

## Acknowledgements

This work was supported by the Welch Foundation through the Welch Endowed Chair to H. C. Z. A-0030. Elements of the TOC graphic were generated with the assistance of Google Gemini.

## References

- 1 C. P. Bryan and G. E. Smith, *Ancient Egyptian medicine: the Papyrus Ebers*, Ares Publishers, Chicago, 1974.
- 2 J. R. Partington, *Origins and Development of Applied Chemistry*, Longmans, Green & Co, London, 1935.
- 3 F. Çeçen and Ö. Aktaş, in *Activated Carbon for Water and Wastewater Treatment*, 2011, pp. 1–11. DOI: [10.1002/9783527639441.ch1](https://doi.org/10.1002/9783527639441.ch1).
- 4 E. M. Diamond and K. T. H. Farrer, Watering The Fleet And The Introduction Of Distillation, *The Mariner's Mirror*, 2005, **91**, 548–553.
- 5 H. Li, M. Eddaoudi, M. O'Keeffe and O. M. Yaghi, Design and synthesis of an exceptionally stable and highly porous metal-organic framework, *Nature*, 1999, **402**, 276.
- 6 S. Kitagawa and M. Kondo, Functional Micropore Chemistry of Crystalline Metal Complex-Assembled Compounds, *Bull. Chem. Soc. Jpn.*, 1998, **71**, 1739–1753.



7 M. Kondo, T. Yoshitomi, H. Matsuzaka, S. Kitagawa and K. Seki, Three-Dimensional Framework with Channeling Cavities for Small Molecules:  $\{[M_2(4,4'-bpy)_3(NO_3)_4] \cdot xH_2O\}_n$  ( $M = Co, Ni, Zn$ ), *Angew. Chem., Int. Ed. Engl.*, 1997, **36**, 1725–1727.

8 M. Eddaoudi, J. Kim, N. Rosi, D. Vodak, J. Wachter, M. Keeffe and O. M. Yaghi, Systematic Design of Pore Size and Functionality in Isoreticular MOFs and Their Application in Methane Storage, *Science*, 2002, **295**, 469.

9 R. Robson, B. F. Abrahams, S. R. Batten, R. W. Gable, B. F. Hoskins and J. Liu, in *Supramolecular Architecture*, American Chemical Society, 1992, vol. 499, ch. 19, pp. 256–273.

10 B. F. Hoskins and R. Robson, Infinite polymeric frameworks consisting of three dimensionally linked rod-like segments, *J. Am. Chem. Soc.*, 1989, **111**, 5962–5964.

11 J. H. Cavka, S. Jakobsen, U. Olsbye, N. Guillou, C. Lamberti, S. Bordiga and K. P. Lillerud, A New Zirconium Inorganic Building Brick Forming Metal Organic Frameworks with Exceptional Stability, *J. Am. Chem. Soc.*, 2008, **130**, 13850–13851.

12 C. Serre, F. Millange, S. Surblé and G. Férey, A Route to the Synthesis of Trivalent Transition-Metal Porous Carboxylates with Trimeric Secondary Building Units, *Angew. Chem., Int. Ed.*, 2004, **43**, 6285–6289.

13 C. T. Lollar, J.-S. Qin, J. Pang, S. Yuan, B. Becker and H.-C. Zhou, Interior Decoration of Stable Metal–Organic Frameworks, *Langmuir*, 2018, **34**, 13795–13807.

14 S. Yuan, L. Feng, K. Wang, J. Pang, M. Bosch, C. Lollar, Y. Sun, J. Qin, X. Yang, P. Zhang, Q. Wang, L. Zou, Y. Zhang, L. Zhang, Y. Fang, J. Li and H.-C. Zhou, Stable Metal–Organic Frameworks: Design, Synthesis, and Applications, *Adv. Mater.*, 2018, **30**, 1704303.

15 S. Yuan, J. S. Qin, C. T. Lollar and H. C. Zhou, Stable Metal–Organic Frameworks with Group 4 Metals: Current Status and Trends, *ACS Cent. Sci.*, 2018, **4**, 440–450.

16 S. Ahn, N. E. Thornburg, Z. Li, T. C. Wang, L. C. Gallington, K. W. Chapman, J. M. Notestein, J. T. Hupp and O. K. Farha, Stable Metal–Organic Framework-Supported Niobium Catalysts, *Inorg. Chem.*, 2016, **55**, 11954–11961.

17 D. Feng, Z.-Y. Gu, J.-R. Li, H.-L. Jiang, Z. Wei and H.-C. Zhou, Zirconium-Metalloporphyrin PCN-222: Mesoporous Metal–Organic Frameworks with Ultrahigh Stability as Biomimetic Catalysts, *Angew. Chem., Int. Ed.*, 2012, **51**, 10307–10310.

18 L. Liu and S. G. Telfer, Systematic Ligand Modulation Enhances the Moisture Stability and Gas Sorption Characteristics of Quaternary Metal–Organic Frameworks, *J. Am. Chem. Soc.*, 2015, **137**, 3901–3909.

19 L. Feng, K.-Y. Wang, X.-L. Lv, J. A. Powell, T.-H. Yan, J. Willman and H.-C. Zhou, Imprinted Apportionment of Functional Groups in Multivariate Metal–Organic Frameworks, *J. Am. Chem. Soc.*, 2019, **141**, 14524–14529.

20 T.-T. Li, Y.-M. Liu, T. Wang, Y.-L. Wu, Y.-L. He, R. Yang and S.-R. Zheng, Regulation of the surface area and surface charge property of MOFs by multivariate strategy: Synthesis, characterization, selective dye adsorption and separation, *Microporous Mesoporous Mater.*, 2018, **272**, 101–108.

21 X.-J. Yu, Y.-M. Xian, C. Wang, H.-L. Mao, M. Kind, T. Abu-Husein, Z. Chen, S.-B. Zhu, B. Ren, A. Terfort and J.-L. Zhuang, Liquid-Phase Epitaxial Growth of Highly Oriented and Multivariate Surface-Attached Metal–Organic Frameworks, *J. Am. Chem. Soc.*, 2019, **141**, 18984–18993.

22 S. Yuan, W. Lu, Y.-P. Chen, Q. Zhang, T.-F. Liu, D. Feng, X. Wang, J. Qin and H.-C. Zhou, Sequential Linker Installation: Precise Placement of Functional Groups in Multivariate Metal–Organic Frameworks, *J. Am. Chem. Soc.*, 2015, **137**, 3177–3180.

23 G. Mouchaham, S. Wang and C. Serre, in *Metal–Organic Frameworks: Applications in Separations and Catalysis*, ed. H. Garcia and S. Navalón, Wiley-VCH, Weinheim, 2018, pp. 1–28.

24 M. Ding, X. Cai and H.-L. Jiang, Improving MOF stability: approaches and applications, *Chem. Sci.*, 2019, **10**, 10209–10230.

25 N. C. Burtch, H. Jasuja and K. S. Walton, Water Stability and Adsorption in Metal–Organic Frameworks, *Chem. Rev.*, 2014, **114**, 10575–10612.

26 Frameworks for commercial success, *Nat. Chem.*, 2016, **8**, 987–987.

27 S. Bose, D. Sengupta, T. M. Rayder, X. Wang, K. O. Kirlikováli, A. K. Sekizkardes, T. Islamoglu and O. K. Farha, Challenges and Opportunities: Metal–Organic Frameworks for Direct Air Capture, *Adv. Funct. Mater.*, 2023, 2307478, DOI: [10.1002/adfm.202307478](https://doi.org/10.1002/adfm.202307478).

28 K. Hoffman, *BASF becomes first company to successfully produce metal-organic frameworks on a commercial scale for carbon capture*, 2023, <https://www.bASF.com/global/en/media/news-releases/2023/10/p-23-327.html>.

29 *Templated Organic Synthesis*, ed. F. Diederich and P. J. Stang, Wiley-VCH, Weinheim, 2000.

30 S. Begum, Z. Hassan, S. Bräse and M. Tsotsalas, Polymerization in MOF-Confined Nanospaces: Tailored Architectures, Functions, and Applications, *Langmuir*, 2020, **36**, 10657–10673.

31 S. Dasgupta and J. Wu, in *Comprehensive Supramolecular Chemistry II*, ed. J. L. Atwood, Elsevier, Oxford, 2017, pp. 251–268. DOI: [10.1016/B978-0-12-409547-2.12588-0](https://doi.org/10.1016/B978-0-12-409547-2.12588-0).

32 Y. Liu, J. Goebel and Y. Yin, Templated synthesis of nanostructured materials, *Chem. Soc. Rev.*, 2013, **42**, 2610–2653.

33 R. R. Poolakkandy and M. M. Menamparambath, Soft-template-assisted synthesis: a promising approach for the fabrication of transition metal oxides, *Nanoscale Adv.*, 2020, **2**, 5015–5045.

34 J. Wang, Y. Wang, H. Hu, Q. Yang and J. Cai, From metal–organic frameworks to porous carbon materials: recent progress and prospects from energy and environmental perspectives, *Nanoscale*, 2020, **12**, 4238–4268.



35 F. Aricó, J. D. Badjic, S. J. Cantrill, A. H. Flood, K. C. F. Leung, Y. Liu and J. F. Stoddart, in *Templates in Chemistry II*, ed. C. A. Schalley, F. Vögtle and K. H. Dötz, Springer Berlin Heidelberg, Berlin, Heidelberg, 2005, pp. 203–259. DOI: [10.1007/b104330](https://doi.org/10.1007/b104330).

36 R. K. O'Reilly, A. J. Turberfield and T. R. Wilks, The Evolution of DNA-Templated Synthesis as a Tool for Materials Discovery, *Acc. Chem. Res.*, 2017, **50**, 2496–2509.

37 L. Oar-Arteta, T. Wezendonk, X. Sun, F. Kapteijn and J. Gascon, Metal organic frameworks as precursors for the manufacture of advanced catalytic materials, *Mater. Chem. Front.*, 2017, **1**, 1709–1745.

38 C. Healy, K. M. Patil, B. H. Wilson, L. Hermanspahn, N. C. Harvey-Reid, B. I. Howard, C. Kleinjan, J. Kolien, F. Payet, S. G. Telfer, P. E. Kruger and T. D. Bennett, The thermal stability of metal-organic frameworks, *Coord. Chem. Rev.*, 2020, **419**, 213388.

39 B. Liu, H. Shioyama, T. Akita and Q. Xu, Metal-Organic Framework as a Template for Porous Carbon Synthesis, *J. Am. Chem. Soc.*, 2008, **130**, 5390–5391.

40 W. Chaikittisilp, K. Ariga and Y. Yamauchi, A new family of carbon materials: synthesis of MOF-derived nanoporous carbons and their promising applications, *J. Mater. Chem. A*, 2013, **1**, 14–19.

41 K. O. Otun, X. Liu and D. Hildebrandt, Metal-organic framework (MOF)-derived catalysts for Fischer-Tropsch synthesis: Recent progress and future perspectives, *J. Energy Chem.*, 2020, **51**, 230–245.

42 V. P. Santos, T. A. Wezendonk, J. J. D. Jaén, A. I. Dugulan, M. A. Nasalevich, H.-U. Islam, A. Chojecki, S. Sartipi, X. Sun, A. A. Hakeem, A. C. J. Koeken, M. Ruitenbeek, T. Davidian, G. R. Meima, G. Sankar, F. Kapteijn, M. Makkee and J. Gascon, Metal organic framework-mediated synthesis of highly active and stable Fischer-Tropsch catalysts, *Nat. Commun.*, 2015, **6**, 6451.

43 J. Du, F. Li and L. Sun, Metal-organic frameworks and their derivatives as electrocatalysts for the oxygen evolution reaction, *Chem. Soc. Rev.*, 2021, **50**, 2663–2695.

44 H.-F. Wang, L. Chen, H. Pang, S. Kaskel and Q. Xu, MOF-derived electrocatalysts for oxygen reduction, oxygen evolution and hydrogen evolution reactions, *Chem. Soc. Rev.*, 2020, **49**, 1414–1448.

45 G. S. Day, J. Li, E. A. Joseph, P. Metz, Z. Perry, M. R. Ryder, K. Page and H.-C. Zhou, Metal oxide decorated porous carbons from controlled calcination of a metal-organic framework, *Nanoscale Adv.*, 2020, **2**, 2758–2767.

46 B. Liu, H. Shioyama, H. Jiang, X. Zhang and Q. Xu, Metal-organic framework (MOF) as a template for syntheses of nanoporous carbons as electrode materials for supercapacitor, *Carbon*, 2010, **48**, 456–463.

47 H.-L. Jiang, B. Liu, Y.-Q. Lan, K. Kuratani, T. Akita, H. Shioyama, F. Zong and Q. Xu, From Metal-Organic Framework to Nanoporous Carbon: Toward a Very High Surface Area and Hydrogen Uptake, *J. Am. Chem. Soc.*, 2011, **133**, 11854–11857.

48 P. Pachfule, B. P. Biswal and R. Banerjee, Control of Porosity by Using Isoreticular Zeolitic Imidazolate Frameworks (IRZIFs) as a Template for Porous Carbon Synthesis, *Chem. – Eur. J.*, 2012, **18**, 11399–11408.

49 J. Hu, H. Wang, Q. Gao and H. Guo, Porous carbons prepared by using metal-organic framework as the precursor for supercapacitors, *Carbon*, 2010, **48**, 3599–3606.

50 L. Chen, J. Bai, C. Wang, Y. Pan, M. Scheer and X. You, One-step solid-state thermolysis of a metal-organic framework: a simple and facile route to large-scale of multi-walled carbon nanotubes, *Chem. Commun.*, 2008, 1581–1583, DOI: [10.1039/B718476J](https://doi.org/10.1039/B718476J).

51 M. Hu, J. Reboul, S. Furukawa, N. L. Torad, Q. Ji, P. Srinivasu, K. Ariga, S. Kitagawa and Y. Yamauchi, Direct Carbonization of Al-Based Porous Coordination Polymer for Synthesis of Nanoporous Carbon, *J. Am. Chem. Soc.*, 2012, **134**, 2864–2867.

52 L. Radhakrishnan, J. Reboul, S. Furukawa, P. Srinivasu, S. Kitagawa and Y. Yamauchi, Preparation of Microporous Carbon Fibers through Carbonization of Al-Based Porous Coordination Polymer (Al-PCP) with Furfuryl Alcohol, *Chem. Mater.*, 2011, **23**, 1225–1231.

53 H. B. Aiyappa, P. Pachfule, R. Banerjee and S. Kurungot, Porous Carbons from Nonporous MOFs: Influence of Ligand Characteristics on Intrinsic Properties of End Carbon, *Cryst. Growth Des.*, 2013, **13**, 4195–4199.

54 S. J. Yang, T. Kim, J. H. Im, Y. S. Kim, K. Lee, H. Jung and C. R. Park, MOF-Derived Hierarchically Porous Carbon with Exceptional Porosity and Hydrogen Storage Capacity, *Chem. Mater.*, 2012, **24**, 464–470.

55 Y. Liu, W. Miao, X. Fang, Y. Tang, D. Wu and S. Mao, MOF-derived metal-free N-doped porous carbon mediated peroxydisulfate activation via radical and non-radical pathways: Role of graphitic N and CO, *Chem. Eng. J.*, 2020, **380**, 122584.

56 R. Luo, J. Wu, J. Zhao, D. Fang, Z. Liu and L. Hu, ZIF-8 derived defect-rich nitrogen-doped carbon with enhanced catalytic activity for efficient non-radical activation of peroxydisulfate, *Environ. Res.*, 2022, **204**, 112060.

57 M. Kim, X. Xu, R. Xin, J. Earnshaw, A. Ashok, J. Kim, T. Park, A. K. Nanjundan, W. A. El-Said, J. W. Yi, J. Na and Y. Yamauchi, KOH-Activated Hollow ZIF-8 Derived Porous Carbon: Nanoarchitected Control for Upgraded Capacitive Deionization and Supercapacitor, *ACS Appl. Mater. Interfaces*, 2021, **13**(44), 52034–52043.

58 K. S. Park, Z. Ni, A. P. Côté, J. Y. Choi, R. Huang, F. J. Uribe-Romo, H. K. Chae, M. O'Keeffe and O. M. Yaghi, Exceptional chemical and thermal stability of zeolitic imidazolate frameworks, *Proc. Natl. Acad. Sci. U. S. A.*, 2006, **103**, 10186–10191.

59 Y.-R. Lee, M.-S. Jang, H.-Y. Cho, H.-J. Kwon, S. Kim and W.-S. Ahn, ZIF-8: A comparison of synthesis methods, *Chem. Eng. J.*, 2015, **271**, 276–280.

60 J. Li, Y. Chen, Y. Tang, S. Li, H. Dong, K. Li, M. Han, Y.-Q. Lan, J. Bao and Z. Dai, Metal-organic framework templated nitrogen and sulfur co-doped porous carbons



as highly efficient metal-free electrocatalysts for oxygen reduction reactions, *J. Mater. Chem. A*, 2014, **2**, 6316–6319.

61 J. Zhang, C. Xu, Y. Zhang, Y. Li, B. Liu, P. Huo, D. Liu and J. Gui, Structural and compositional analysis of MOF-derived carbon nanomaterials for the oxygen reduction reaction, *Chem. Commun.*, 2024, **60**, 2572–2590.

62 D. Wang, H. Liu, Z. Cao, T. Cai, P. Han, J. Song, L. Kong and C. Liu, Ordered porous nitrogen-doped carbon with atomically dispersed FeN<sub>4</sub> for efficient oxygen reduction reaction in microbial fuel cell, *Sci. Total Environ.*, 2022, **838**, 156186.

63 S. Xu, A. Dong, Y. Hu, Z. Yang, S. Huang and J. Qian, Multidimensional MOF-derived carbon nanomaterials for multifunctional applications, *J. Mater. Chem. A*, 2023, **11**, 9721–9747.

64 L. Chai, X. Wang, Y. Hu, X. Li, S. Huang, J. Pan, J. Qian and X. Sun, In-MOF-Derived Hierarchically Hollow Carbon Nanostraws for Advanced Zinc-Iodine Batteries, *Adv. Sci.*, 2022, **9**, 2105063.

65 H. F. Drake, G. S. Day, S. W. Vali, Z. Xiao, S. Banerjee, J. Li, E. A. Joseph, J. E. Kusznyski, Z. T. Perry, A. Kirchon, O. K. Ozdemir, P. A. Lindahl and H.-C. Zhou, The thermally induced decarboxylation mechanism of a mixed-oxidation state carboxylate-based iron metal-organic framework, *Chem. Commun.*, 2019, **55**, 12769–12772.

66 H. F. Drake, Z. Xiao, G. S. Day, S. W. Vali, W. Chen, Q. Wang, Y. Huang, T.-H. Yan, J. E. Kusznyski, P. A. Lindahl, M. R. Ryder and H.-C. Zhou, Thermal decarboxylation for the generation of hierarchical porosity in isostructural metal-organic frameworks containing open metal sites, *Mater. Adv.*, 2021, **2**, 5487–5493.

67 Y. Tan, K. Zhu, D. Li, F. Bai, Y. Wei and P. Zhang, N-doped graphene/Fe–Fe<sub>3</sub>C nano-composite synthesized by a Fe-based metal organic framework and its anode performance in lithium ion batteries, *Chem. Eng. J.*, 2014, **258**, 93–100.

68 J. Chen and J. Qian, Insights on MOF-derived metal–carbon nanostructures for oxygen evolution, *Dalton Trans.*, 2024, **53**, 2903–2916.

69 Q. Ren, H. Wang, X.-F. Lu, Y.-X. Tong and G.-R. Li, Recent Progress on MOF-Derived Heteroatom-Doped Carbon-Based Electrocatalysts for Oxygen Reduction Reaction, *Adv. Sci.*, 2018, **5**, 1700515.

70 N. Lu, X. Zhang, X. Yan, D. Pan, B. Fan and R. Li, Synthesis of novel mesoporous sulfated zirconia nanosheets derived from Zr-based metal-organic frameworks, *CrystEngComm*, 2020, **22**, 44–51.

71 X. Yan, N. Lu, B. Fan, J. Bao, D. Pan, M. Wang and R. Li, Synthesis of mesoporous and tetragonal zirconia with inherited morphology from metal-organic frameworks, *CrystEngComm*, 2015, **17**, 6426–6433.

72 S. Ni and Y. Li, t-ZrO<sub>2</sub> prepared by a novel zirconium oxalate synthesised solvothermally, *Micro-Nano Lett.*, 2018, **13**, 919–922.

73 C. Wang, J. Kim, J. Tang, M. Kim, H. Lim, V. Malgras, J. You, Q. Xu, J. Li and Y. Yamauchi, New Strategies for Novel MOF-Derived Carbon Materials Based on Nanoarchitectures, *Chem.*, 2020, **6**, 19–40.

74 J. Ren, Y. Huang, H. Zhu, B. Zhang, H. Zhu, S. Shen, G. Tan, F. Wu, H. He, S. Lan, X. Xia and Q. Liu, Recent progress on MOF-derived carbon materials for energy storage, *Carbon Energy*, 2020, **2**, 176–202.

75 N. L. Torad, M. Hu, S. Ishihara, H. Sukegawa, A. A. Belik, M. Imura, K. Ariga, Y. Sakka and Y. Yamauchi, Direct Synthesis of MOF-Derived Nanoporous Carbon with Magnetic Co Nanoparticles toward Efficient Water Treatment, *Small*, 2014, **10**, 2096–2107.

76 A. I. Cherevko, I. A. Nikovskiy, Y. V. Nelyubina, K. M. Skupov, N. N. Efimov and V. V. Novikov, 3D-Printed Porous Magnetic Carbon Materials Derived from Metal-Organic Frameworks, *Polymers*, 2021, **13**(22), 3881, DOI: [10.3390/polym13223881](https://doi.org/10.3390/polym13223881).

77 P. Yin, T. Yao, Y. Wu, L. Zheng, Y. Lin, W. Liu, H. Ju, J. Zhu, X. Hong, Z. Deng, G. Zhou, S. Wei and Y. Li, Single Cobalt Atoms with Precise N-Coordination as Superior Oxygen Reduction Reaction Catalysts, *Angew. Chem., Int. Ed.*, 2016, **55**, 10800–10805.

78 J. Hwang, A. Ejsmont, R. Freund, J. Goscianska, B. V. K. J. Schmidt and S. Wuttke, Controlling the morphology of metal-organic frameworks and porous carbon materials: metal oxides as primary architecture-directing agents, *Chem. Soc. Rev.*, 2020, **49**, 3348–3422.

79 N. Kitchamsetti and J. S. Cho, A roadmap of MOFs derived porous carbon, oxides, chalcogenides, and phosphides of metals: Synthesis, properties, parameter modulation and their utilization as an electrode for Li/Na/K-ion batteries, *J. Energy Storage*, 2024, **84**, 110947.

80 Y. Dai, P. Lu, Z. Cao, C. T. Campbell and Y. Xia, The physical chemistry and materials science behind sinter-resistant catalysts, *Chem. Soc. Rev.*, 2018, **47**, 4314–4331.

81 G. I. Finch and K. P. Sinha, On Reaction in the Solid State, *Proc. R. Soc. London, Ser. A*, 1957, **239**, 145–153.

82 Z. Zhou, J. Zhang, S. Mukherjee, S. Hou, R. Khare, M. Döblinger, O. Tomanec, M. Otyepka, M. Koch, P. Gao, L. Zhou, W. Li and R. A. Fischer, Porphyrinic MOF derived Single-atom electrocatalyst enables methanol oxidation, *Chem. Eng. J.*, 2022, **449**, 137888.

83 Y. Hu, C. Li, S. Xi, Z. Deng, X. Liu, A. K. Cheetham and J. Wang, Direct Pyrolysis of a Manganese-Triazolate Metal-Organic Framework into Air-Stable Manganese Nitride Nanoparticles, *Adv. Sci.*, 2021, **8**, 2003212.

84 G. S. Day, H. F. Drake, A. Contreras-Ramirez, M. R. Ryder, K. Page and H.-C. Zhou, Controlled Metal Oxide and Porous Carbon Temptation Using Metal-Organic Frameworks, *Cryst. Growth Des.*, 2021, **21**, 4249–4258.

85 Y.-W. Li, W.-J. Zhang, J. Li, H.-Y. Ma, H.-M. Du, D.-C. Li, S.-N. Wang, J.-S. Zhao, J.-M. Dou and L. Xu, Fe-MOF-Derived Efficient ORR/OER Bifunctional Electrocatalyst for Rechargeable Zinc–Air Batteries, *ACS Appl. Mater. Interfaces*, 2020, **12**, 44710–44719.

86 H. Zheng, N. Xu, B. Hou, X. Zhao, M. Dong, C. Sun, X.-L. Wang and Z.-M. Su, Bimetallic Metal-Organic



Framework-Derived Graphitic Carbon-Coated Small Co/VN Nanoparticles as Advanced Trifunctional Electrocatalysts, *ACS Appl. Mater. Interfaces*, 2021, **13**, 2462–2471.

87 R. Das, P. Pachfule, R. Banerjee and P. Poddar, Metal and metal oxide nanoparticle synthesis from metal organic frameworks (MOFs): finding the border of metal and metal oxides, *Nanoscale*, 2012, **4**, 591–599.

88 S. Payra, N. Devaraj, K. Tarafder and S. Roy, Unprecedented Electroreduction of  $\text{CO}_2$  over Metal Organic Framework-Derived Intermetallic Nano-Alloy  $\text{Cu}_{0.85}\text{Ni}_{0.15}/\text{C}$ , *ACS Appl. Energy Mater.*, 2022, **5**, 4945–4955.

89 Q. Zhang, X. Zhang, D. Lei, S. Qiao, Q. Wang, X. Shi, C. Huang, G. He and F. Zhang, MOF-Derived Hollow Carbon Supported Nickel-Cobalt Alloy Catalysts Driving Fast Polysulfide Conversion for Lithium-Sulfur Batteries, *ACS Appl. Mater. Interfaces*, 2023, **15**, 15377–15386.

90 F. Zheng, D. Zhu, X. Shi and Q. Chen, Metal-organic framework-derived porous  $\text{Mn}_{1.8}\text{Fe}_{1.2}\text{O}_4$  nanocubes with an interconnected channel structure as high-performance anodes for lithium ion batteries, *J. Mater. Chem. A*, 2015, **3**, 2815–2824.

91 H. Guo, T. Li, W. Chen, L. Liu, X. Yang, Y. Wang and Y. Guo, General design of hollow porous  $\text{CoFe}_2\text{O}_4$  nanocubes from metal-organic frameworks with extraordinary lithium storage, *Nanoscale*, 2014, **6**, 15168–15174.

92 Z. Du, F. Chen, S. Fang, X. Yang, Y. Ge, K. Shurtz, H.-C. Zhou, Y. H. Hu and Y. Li, Engineering Bimetallic Ni-Cu Nanoparticles Confined in MOF-Derived Nanocomposite for Efficient Dry Reforming of Methane, *ES Energy Environ.*, 2024, **23**, 1097.

93 J. B. DeCoste, G. W. Peterson, H. Jasuja, T. G. Glover, Y.-G. Huang and K. S. Walton, Stability and degradation mechanisms of metal-organic frameworks containing the  $\text{Zr}_6\text{O}_4(\text{OH})_4$  secondary building unit, *J. Mater. Chem. A*, 2013, **1**, 5642–5650.

94 Z. Chen, Z. Chen, O. K. Farha and K. W. Chapman, Mechanistic Insights into Nanoparticle Formation from Bimetallic Metal-Organic Frameworks, *J. Am. Chem. Soc.*, 2021, **143**, 8976–8980.

95 A. E. Platero-Prats, A. Mavrandakis, L. C. Gallington, Y. Liu, J. T. Hupp, O. K. Farha, C. J. Cramer and K. W. Chapman, Structural Transitions of the Metal-Oxide Nodes within Metal-Organic Frameworks: On the Local Structures of NU-1000 and UiO-66, *J. Am. Chem. Soc.*, 2016, **138**, 4178–4185.

96 M. Folkjær, L. F. Lundgaard, H. S. Jeppesen, M. J. Marks, M. S. Hvid, S. Frank, G. Cibin and N. Lock, Pyrolysis of a metal-organic framework followed by in situ X-ray absorption spectroscopy, powder diffraction and pair distribution function analysis, *Dalton Trans.*, 2022, **51**, 10740–10750.

97 J. A. Powell, H. Lin, Y.-C. Hsu, D. E. Young and H.-C. Zhou, Exploitation of MOF decomposition mechanisms to tailor MOF-derived carbon structure in mono- and multimetallic PCN-250, *Cryst. Growth Des.*, 2025, DOI: [10.1021/acs.cgd.4c01690](https://doi.org/10.1021/acs.cgd.4c01690).

98 P. Yang, X. Song, C. Jia and H.-S. Chen, Metal-organic framework-derived hierarchical  $\text{ZnO}/\text{NiO}$  composites: Morphology, microstructure and electrochemical performance, *J. Ind. Eng. Chem.*, 2018, **62**, 250–257.

99 P. Ge, H. Hou, S. Li, L. Yang and X. Ji, Tailoring Rod-Like  $\text{FeSe}_2$  Coated with Nitrogen-Doped Carbon for High-Performance Sodium Storage, *Adv. Funct. Mater.*, 2018, **28**, 1801765.

100 S. Tsunekawa, S. Ito, Y. Kawazoe and J. T. Wang, Critical Size of the Phase Transition from Cubic to Tetragonal in Pure Zirconia Nanoparticles, *Nano Lett.*, 2003, **3**, 871–875.

101 Y.-Z. Chen, C. Wang, Z.-Y. Wu, Y. Xiong, Q. Xu, S.-H. Yu and H.-L. Jiang, From Bimetallic Metal-Organic Framework to Porous Carbon: High Surface Area and Multicomponent Active Dopants for Excellent Electrocatalysis, *Adv. Mater.*, 2015, **27**, 5010–5016.

102 B. You, N. Jiang, M. Sheng, W. S. Drisdell, J. Yano and Y. Sun, Bimetal-Organic Framework Self-Adjusted Synthesis of Support-Free Nonprecious Electrocatalysts for Efficient Oxygen Reduction, *ACS Catal.*, 2015, **5**, 7068–7076.

103 H. Wang, Y. Wang, Y. Li, X. Lan, B. Ali and T. Wang, Highly Efficient Hydrogenation of Nitroarenes by N-Doped Carbon-Supported Cobalt Single-Atom Catalyst in Ethanol/Water Mixed Solvent, *ACS Appl. Mater. Interfaces*, 2020, **12**, 34021–34031.

104 S. Gong, C. Wang, P. Jiang, L. Hu, H. Lei and Q. Chen, Designing highly efficient dual-metal single-atom electrocatalysts for the oxygen reduction reaction inspired by biological enzyme systems, *J. Mater. Chem. A*, 2018, **6**, 13254–13262.

105 H. Li, X. Chen, J. Chen, K. Shen and Y. Li, Hierarchically porous Fe,N-doped carbon nanorods derived from 1D Fe-doped MOFs as highly efficient oxygen reduction electrocatalysts in both alkaline and acidic media, *Nanoscale*, 2021, **13**, 10500–10508.

106 W. Yang, P. Hong, D. Yang, Y. Yang, Z. Wu, C. Xie, J. He, K. Zhang, L. Kong and J. Liu, Enhanced Fenton-like degradation of sulfadiazine by single atom iron materials fixed on nitrogen-doped porous carbon, *J. Colloid Interface Sci.*, 2021, **597**, 56–65.

107 L. Jiao, J. Zhu, Y. Zhang, W. Yang, S. Zhou, A. Li, C. Xie, X. Zheng, W. Zhou, S.-H. Yu and H.-L. Jiang, Non-Bonding Interaction of Neighboring Fe and Ni Single-Atom Pairs on MOF-Derived N-Doped Carbon for Enhanced  $\text{CO}_2$  Electroreduction, *J. Am. Chem. Soc.*, 2021, **143**, 19417–19424.

108 F. Pan, H. Zhang, Z. Liu, D. Cullen, K. Liu, K. More, G. Wu, G. Wang and Y. Li, Atomic-level active sites of efficient imidazolate framework-derived nickel catalysts for  $\text{CO}_2$  reduction, *J. Mater. Chem. A*, 2019, **7**, 26231–26237.

109 P. Yue, K. Xiong, L. Ma, J. Li, L. Zhang, X. Zhu, Q. Fu and Q. Liao, MOF-Derived Ni Single-Atom Catalyst with Abundant Mesopores for Efficient Mass Transport in Electrolytic Bicarbonate Conversion, *ACS Appl. Mater. Interfaces*, 2022, **14**, 54840–54847.



110 H. Cheng, X. Wu, M. Feng, X. Li, G. Lei, Z. Fan, D. Pan, F. Cui and G. He, Atomically Dispersed Ni/Cu Dual Sites for Boosting the CO<sub>2</sub> Reduction Reaction, *ACS Catal.*, 2021, **11**, 12673–12681.

111 S.-M. Li, Y. Shi, J.-J. Zhang, Y. Wang, H. Wang and J.-X. Lu, Atomically Dispersed Copper on N-Doped Carbon Nanosheets for Electrocatalytic Synthesis of Carbamates from CO<sub>2</sub> as a C<sub>1</sub> Source, *ChemSusChem*, 2021, **14**, 2050–2055.

112 X. Cao, R. Tong, S. Tang, B. W. L. Jang, A. Mirjalili, J. Li, X. Guo, J. Zhang, J. Hu and X. Meng, Design of Pd-Zn Bimetal MOF Nanosheets and MOF-Derived Pd<sub>3.9</sub>Zn<sub>6.1</sub>/CNS Catalyst for Selective Hydrogenation of Acetylene under Simulated Front-End Conditions, *Molecules*, 2022, **27**(17), 5736.

113 T.-H. Yang, P.-C. Han, I. T. Wang, C. H. Chen, M. A. M. Khan, C.-Y. Wen and K. C. W. Wu, Water-Based Synthesis of Gold Single Atoms-Embedded, Metal-Organic Frameworks-Derived Nanoporous Carbon Nanoparticles with Enhanced Reduction Ability, *Adv. Mater. Interfaces*, 2021, **8**, 2001638.

114 N. Du, C. Wang, R. Long and Y. Xiong, N-doped carbon-stabilized PtCo nanoparticles derived from Pt@ZIF-67: Highly active and durable catalysts for oxygen reduction reaction, *Nano Res.*, 2017, **10**, 3228–3237.

115 Z. Qi, Y. Pei, T. W. Goh, Z. Wang, X. Li, M. Lowe, R. V. Maligal-Ganesh and W. Huang, Conversion of confined metal@ZIF-8 structures to intermetallic nanoparticles supported on nitrogen-doped carbon for electrocatalysis, *Nano Res.*, 2018, **11**, 3469–3479.

116 X. X. Wang, S. Hwang, Y.-T. Pan, K. Chen, Y. He, S. Karakalos, H. Zhang, J. S. Spendelow, D. Su and G. Wu, Ordered Pt<sub>3</sub>Co Intermetallic Nanoparticles Derived from Metal–Organic Frameworks for Oxygen Reduction, *Nano Lett.*, 2018, **18**, 4163–4171.

117 D. B. Christensen, R. L. Mortensen, S. Kramer and S. Kegnæs, Study of CoCu Alloy Nanoparticles Supported on MOF-Derived Carbon for Hydrosilylation of Ketones, *Catal. Lett.*, 2020, **150**, 1537–1545.

118 A. Almasoudi and R. Mokaya, Preparation and hydrogen storage capacity of templated and activated carbons nano-cast from commercially available zeolitic imidazolate framework, *J. Mater. Chem.*, 2012, **22**, 146–152.

119 A. Banerjee, R. Gokhale, S. Bhatnagar, J. Jog, M. Bhardwaj, B. Lefez, B. Hannoyer and S. Ogale, MOF derived porous carbon–Fe<sub>3</sub>O<sub>4</sub> nanocomposite as a high performance, recyclable environmental superadsorbent, *J. Mater. Chem.*, 2012, **22**, 19694–19699.

120 Z. Hasan, D.-W. Cho, I.-H. Nam, C.-M. Chon and H. Song, Preparation of calcined zirconia-carbon composite from metal organic frameworks and its application to adsorption of crystal violet and salicylic acid, *Materials*, 2016, **9**, 261.

121 B. Chen, X. Zhang, Y. Liu, X. Ma, X. Wang, X. Cao and L. Lian, Magnetic porous carbons derived from iron-based metal-organic framework loaded with glucose for effective extraction of synthetic organic dyes in drinks, *J. Chromatogr. A*, 2022, **1661**, 462716.

122 M. Yu, H. Dong, Y. Zheng and W. Liu, Ternary metal oxide embedded carbon derived from metal organic frameworks for adsorption of methylene blue and acid red 73, *Chemosphere*, 2021, **280**, 130567.

123 A. Fu, Z. Liu and Z. Sun, Cu/Fe oxide integrated on graphite felt for degradation of sulfamethoxazole in the heterogeneous electro-Fenton process under near-neutral conditions, *Chemosphere*, 2022, **297**, 134257.

124 B. N. Bhadra, N. A. Khan and S. H. Jhung, Co supported on N-doped carbon, derived from bimetallic azolate framework-6: a highly effective oxidative desulfurization catalyst, *J. Mater. Chem. A*, 2019, **7**, 17823–17833.

125 J. Cao, Z. Yang, W. Xiong, Y. Zhou, Y. Wu, M. Jia, S. Sun, C. Zhou, Y. Zhang and R. Zhong, Peroxymonosulfate activation of magnetic Co nanoparticles relative to an N-doped porous carbon under confinement: Boosting stability and performance, *Sep. Purif. Technol.*, 2020, **250**, 117237.

126 S. Zhao, S. Li, Y. Long, X. Shen, Z. Zhao, Q. Wei, S. Wang, Z. Zhang, X. Zhang and Z. Zhang, Ce-based Heterogeneous Catalysts by Partial Thermal Decomposition of Ce-MOFs in Activation of Peroxymonosulfate for the Removal of Organic Pollutants under Visible Light, *Chemosphere*, 2021, **130637**, DOI: [10.1016/j.chemosphere.2021.130637](https://doi.org/10.1016/j.chemosphere.2021.130637).

127 T. A. Wezendonk, Q. S. E. Warringa, V. P. Santos, A. Chojecki, M. Ruitenbeek, G. Meima, M. Makkee, F. Kapteijn and J. Gascon, Structural and elemental influence from various MOFs on the performance of Fe@C catalysts for Fischer–Tropsch synthesis, *Faraday Discuss.*, 2017, **197**, 225–242.

128 Q. Zhao, S. Huang, X. Han, J. Chen, J. Wang, A. Rykov, Y. Wang, M. Wang, J. Lv and X. Ma, Highly active and controllable MOF-derived carbon nanosheets supported iron catalysts for Fischer-Tropsch synthesis, *Carbon*, 2021, **173**, 364–375.

129 A. Shahzad, F. Zulfiqar and M. Arif Nadeem, Cobalt containing bimetallic ZIFs and their derivatives as OER electrocatalysts: A critical review, *Coord. Chem. Rev.*, 2023, **477**, 214925.

130 Y. Song, C. Yu, D. Ma and K. Liu, Recent progress on ZIF-8 based MOF derivatives for electrocatalysis, *Coord. Chem. Rev.*, 2024, **499**, 215492.

131 L. Chai, R. Li, Y. Sun, K. Zhou and J. Pan, MOF-derived Carbon-Based Materials for Energy-Related Applications, *Adv. Mater.*, 2025, 2413658.

132 B. Han, J. Liu, C. Lee, C. Lv and Q. Yan, Recent Advances in Metal-Organic Framework-Based Nanomaterials for Electrocatalytic Nitrogen Reduction, *Small Methods*, 2023, **7**, 2300277.

133 S. Luo, X. Li, B. Zhang, Z. Luo and M. Luo, MOF-Derived Co<sub>3</sub>O<sub>4</sub>@NC with Core–Shell Structures for N<sub>2</sub> Electrochemical Reduction under Ambient Conditions, *ACS Appl. Mater. Interfaces*, 2019, **11**, 26891–26897.

134 T. Zhu, Q. Chen, P. Liao, W. Duan, S. Liang, Z. Yan and C. Feng, Single-Atom Cu Catalysts for Enhanced



Electrocatalytic Nitrate Reduction with Significant Alleviation of Nitrite Production, *Small*, 2020, **16**, 2004526.

135 S. Zhang, M. Li, J. Li, Q. Song and X. Liu, High-ammonia selective metal-organic framework-derived Co-doped Fe/Fe<sub>2</sub>O<sub>3</sub> catalysts for electrochemical nitrate reduction, *Proc. Natl. Acad. Sci. U. S. A.*, 2022, **119**, e2115504119.

136 F. Wang, L. Zhang, T. Wang, F. Zhang, Q. Liu, H. Zhao, B. Zheng, J. Du and X. Sun, In Situ Derived Bi Nanoparticles Confined in Carbon Rods as an Efficient Electrocatalyst for Ambient N<sub>2</sub> Reduction to NH<sub>3</sub>, *Inorg. Chem.*, 2021, **60**, 7584–7589.

137 S. Yang, J. Zhang, L. Peng, M. Asgari, D. Stoian, I. Kochetygov, W. Luo, E. Oveisi, O. Trukhina, A. H. Clark, D. T. Sun and W. L. Queen, A metal-organic framework/polymer derived catalyst containing single-atom nickel species for electrocatalysis, *Chem. Sci.*, 2020, **11**, 10991–10997.

138 K. Zhao, Y. Liu, X. Quan, S. Chen and H. Yu, CO<sub>2</sub> Electroreduction at Low Overpotential on Oxide-Derived Cu/Carbons Fabricated from Metal Organic Framework, *ACS Appl. Mater. Interfaces*, 2017, **9**, 5302–5311.

139 X. Feng, F. Pan, P. Zhang, X. Wang, H.-C. Zhou, Y. Huang and Y. Li, Metal-Organic Framework MIL-125 Derived Mg<sup>2+</sup>-Doped Mesoporous TiO<sub>2</sub> for Photocatalytic CO<sub>2</sub> Reduction, *ChemPhotoChem*, 2021, **5**, 79–89.

140 J. Castells-Gil, S. Ould-Chikh, A. Ramírez, R. Ahmad, G. Prieto, A. R. Gómez, L. Garzón-Tovar, S. Telalovic, L. Liu, A. Genovese, N. M. Padial, A. Aguilar-Tapia, P. Bordet, L. Cavallo, C. Martí-Gastaldo and J. Gascon, Unlocking mixed oxides with unprecedented stoichiometries from heterometallic metal-organic frameworks for the catalytic hydrogenation of CO<sub>2</sub>, *Chem. Catal.*, 2021, **1**, 364–382.

141 S. Zhao, H. Yin, L. Du, L. He, K. Zhao, L. Chang, G. Yin, H. Zhao, S. Liu and Z. Tang, Carbonized Nanoscale Metal-Organic Frameworks as High Performance Electrocatalyst for Oxygen Reduction Reaction, *ACS Nano*, 2014, **8**, 12660–12668.

142 Y. Chen, R. Gao, S. Ji, H. Li, K. Tang, P. Jiang, H. Hu, Z. Zhang, H. Hao, Q. Qu, X. Liang, W. Chen, J. Dong, D. Wang and Y. Li, Atomic-Level Modulation of Electronic Density at Cobalt Single-Atom Sites Derived from Metal-Organic Frameworks: Enhanced Oxygen Reduction Performance, *Angew. Chem., Int. Ed.*, 2021, **60**, 3212–3221.

143 Y. Yin, J. Wang, T. Li, J. P. Hill, A. Rowan, Y. Sugahara and Y. Yamauchi, Nanoarchitecturing Carbon Nanodot Arrays on Zeolitic Imidazolate Framework-Derived Cobalt-Nitrogen-Doped Carbon Nanoflakes toward Oxygen Reduction Electrocatalysts, *ACS Nano*, 2021, **15**, 13240–13248.

144 W. Zhang, X. Yao, S. Zhou, X. Li, L. Li, Z. Yu and L. Gu, ZIF-8/ZIF-67-Derived Co-N-Embedded 1D Porous Carbon Nanofibers with Graphitic Carbon-Encased Co Nanoparticles as an Efficient Bifunctional Electrocatalyst, *Small*, 2018, **14**, 1800423.

145 Z. Wang, H. Jin, T. Meng, K. Liao, W. Meng, J. Yang, D. He, Y. Xiong and S. Mu, Fe, Cu-Coordinated ZIF-Derived Carbon Framework for Efficient Oxygen Reduction Reaction and Zinc–Air Batteries, *Adv. Funct. Mater.*, 2018, **28**, 1802596.

146 X. Xie, L. Peng, H. Yang, G. I. N. Waterhouse, L. Shang and T. Zhang, MIL-101-Derived Mesoporous Carbon Supporting Highly Exposed Fe Single-Atom Sites as Efficient Oxygen Reduction Reaction Catalysts, *Adv. Mater.*, 2021, **33**, 2101038.

147 S. Yuan, J. Zhang, L. Hu, J. Li, S. Li, Y. Gao, Q. Zhang, L. Gu, W. Yang, X. Feng and B. Wang, Decarboxylation-Induced Defects in MOF-Derived Single Cobalt Atom@Carbon Electrocatalysts for Efficient Oxygen Reduction, *Angew. Chem., Int. Ed.*, 2021, **60**, 21685–21690.

148 J. Song, C. Wei, Z.-F. Huang, C. Liu, L. Zeng, X. Wang and Z. J. Xu, A review on fundamentals for designing oxygen evolution electrocatalysts, *Chem. Soc. Rev.*, 2020, **49**, 2196–2214.

149 A. Parkash, Metal-organic framework derived ultralow-loading platinum-copper catalyst: a highly active and durable bifunctional electrocatalyst for oxygen-reduction and evolution reactions, *Nanotechnology*, 2021, **32**, 325703.

150 J. W. Sturman, M. S. E. Houache, W. D. do Pim, E. A. Baranova, M. Murugesu and Y. Abu-Lebdeh, Critical Investigation of Metal-Organic-Frameworks to Improve the Silicon Anode of Lithium-Ion Batteries, *ACS Appl. Energy Mater.*, 2024, **7**, 21–30.

151 R. Kaur, V. A. Chhabra, V. Chaudhary, K. Vikrant, S. K. Tripathi, Y. Su, P. Kumar, K.-H. Kim and A. Deep, Metal-organic frameworks and their derivatives as anode material in lithium-ion batteries: Recent advances towards novel configurations, *Int. J. Energy Res.*, 2022, **46**, 13178–13204.

152 G. Chu, C. Wang, Z. Yang, L. Qin and X. Fan, MOF-derived porous graphitic carbon with optimized plateau capacity and rate capability for high performance lithium-ion capacitors, *Int. J. Miner., Metall. Mater.*, 2024, **31**, 395–404.

153 K. Xue, Y. Si, S. Xie, J. Yang, Y. Mo, B. Long, W. Wei, P. Cao, H. Wei, H. Guan, E. G. Michaelis, G. Guo, Y. Yue and C. Shan, Free-Standing N-Doped Porous Carbon Fiber Membrane Derived From Zn-MOF-74: Synthesis and Application as Anode for Sodium-Ion Battery With an Excellent Performance, *Front. Chem.*, 2021, **9**, 647545.

154 R. Tian, S.-H. Park, P. J. King, G. Cunningham, J. Coelho, V. Nicolosi and J. N. Coleman, Quantifying the factors limiting rate performance in battery electrodes, *Nat. Commun.*, 2019, **10**, 1933.

155 A. Li, Y. Tong, B. Cao, H. Song, Z. Li, X. Chen, J. Zhou, G. Chen and H. Luo, MOF-derived multifractal porous carbon with ultrahigh lithium-ion storage performance, *Sci. Rep.*, 2017, **7**, 40574.

156 Y. Li, J. Zhang and M. Chen, MOF-derived carbon and composites as advanced anode materials for potassium



ion batteries: A review, *Sustainable Mater. Technol.*, 2020, **26**, e00217.

157 Y. Zhang, M. Sha, Q. Fu, H. Zhao and Y. Lei, An overview of metal-organic frameworks-derived carbon as anode materials for sodium- and potassium-ion batteries, *Mater. Today Sustain.*, 2022, **18**, 100156.

158 C. K. Chan, H. Peng, G. Liu, K. McIlwrath, X. F. Zhang, R. A. Huggins and Y. Cui, High-performance lithium battery anodes using silicon nanowires, *Nat. Nanotechnol.*, 2008, **3**, 31–35.

159 M. Ko, S. Chae, J. Ma, N. Kim, H.-W. Lee, Y. Cui and J. Cho, Scalable synthesis of silicon-nanolayer-embedded graphite for high-energy lithium-ion batteries, *Nat. Energy*, 2016, **1**, 1–8.

160 B. Chen, L. Chen, L. Zu, Y. Feng, Q. Su, C. Zhang and J. Yang, Zero-Strain High-Capacity Silicon/Carbon Anode Enabled by a MOF-Derived Space-Confined Single-Atom Catalytic Strategy for Lithium-Ion Batteries, *Adv. Mater.*, 2022, **34**, 2200894.

161 R. Gao, J. Tang, X. Yu, S. Tang, K. Ozawa, T. Sasaki and L.-C. Qin, In situ synthesis of MOF-derived carbon shells for silicon anode with improved lithium-ion storage, *Nano Energy*, 2020, **70**, 104444.

162 Y.-J. Qiao, H. Zhang, Y.-X. Hu, W.-P. Li, W.-J. Liu, H.-M. Shang, M.-Z. Qu, G.-C. Peng and Z.-W. Xie, A chain-like compound of Si@CNT nanostructures and MOF-derived porous carbon as an anode for Li-ion batteries, *Int. J. Miner., Metall. Mater.*, 2021, **28**, 1611.

163 H. Deng, S. Grunder, K. E. Cordova, C. Valente, H. Furukawa, M. Hmadeh, F. Gándara, A. C. Whalley, Z. Liu, S. Asahina, H. Kazumori, M. O'Keeffe, O. Terasaki, J. F. Stoddart and O. M. Yaghi, Large-Pore Apertures in a Series of Metal-Organic Frameworks, *Science*, 2012, **336**, 1018.

164 J. Hou, M. L. Ríos Gómez, A. Krajnc, A. McCaul, S. Li, A. M. Bumstead, A. F. Sapnik, Z. Deng, R. Lin, P. A. Chater, D. S. Keeble, D. A. Keen, D. Appadoo, B. Chan, V. Chen, G. Mali and T. D. Bennett, Halogenated Metal–Organic Framework Glasses and Liquids, *J. Am. Chem. Soc.*, 2020, **142**, 3880–3890.

165 M. A. Sayeed and A. P. O'Mullane, Electrodeposition at Highly Negative Potentials of an Iron-Cobalt Oxide Catalyst for Use in Electrochemical Water Splitting, *ChemPhysChem*, 2019, **20**, 3112–3119.

166 M. Giménez-Marqués, A. Santiago-Portillo, S. Navalón, M. Álvaro, V. Briois, F. Nouar, H. Garcia and C. Serre, Exploring the catalytic performance of a series of bi-metallic MIL-100(Fe, Ni) MOFs, *J. Mater. Chem. A*, 2019, **7**, 20285–20292.

167 L. J. Wang, H. Deng, H. Furukawa, F. Gándara, K. E. Cordova, D. Peri and O. M. Yaghi, Synthesis and Characterization of Metal–Organic Framework-74 Containing 2, 4, 6, 8, and 10 Different Metals, *Inorg. Chem.*, 2014, **53**, 5881–5883.

168 D. Capková, T. Kazda, O. Čech, N. Király, T. Zelenka, P. Čudek, A. Sharma, V. Hornebecq, A. S. Fedorková and M. Almáši, Influence of metal-organic framework MOF-76 (Gd) activation/carbonization on the cycle performance stability in Li-S battery, *J. Energy Storage*, 2022, **51**, 104419.

169 C.-H. Liu, E. M. Janke, R. Li, P. Juhás, O. Gang, D. V. Talapin and S. J. Billinge, sasPDF: pair distribution function analysis of nanoparticle assemblies from small-angle scattering data, *J. Appl. Crystallogr.*, 2020, **53**, 699–709.

170 N. Allasia, S. M. Collins, Q. M. Ramasse and G. Vilé, Hidden Impurities Generate False Positives in Single Atom Catalyst Imaging, *Angew. Chem., Int. Ed.*, 2024, **63**, e202404883.

